Exploration of the diagnostic value and molecular mechanism of miR-1 in prostate cancer: A study based on meta-analyses and bioinformatics

ZU-CHENG XIE[1], JIA-CHENG HUANG[1], LI-JIE ZHANG[2], BIN-LIANG GAN[3], DONG-YUE WEN[2], GANG CHEN[2], SHENG-HUA LI[1] and HAI-BIAO YAN[1]

Departments of [1]Urological Surgery, [2]Pathology and [3]Medical Oncology, The First Affiliated Hospital of Guangxi Medical University, Nanning, Guangxi Zhuang Autonomous Region 530021, P.R. China

Received December 17, 2017; Accepted September 24, 2018

DOI: 10.3892/mmr.2018.9598

Abstract. Prostate cancer (PCa) remains a principal issue to be addressed in male cancer-associated mortality. Therefore, the present study aimed to examine the clinical value and associated molecular mechanism of microRNA (miR)-1 in PCa. A meta-analysis was conducted to evaluate the diagnosis of miR-1 in PCa via Gene Expression Omnibus and ArrayExpress datasets, The Cancer Genome Atlas miR-1 expression data and published literature. It was identified that expression of miR-1 was significantly downregulated in PCa. Decreased miR-1 expression possessed moderate diagnostic value, with area under the curve, sensitivity, specificity and odds ratio values at 0.73, 0.77, 0.57 and 4.60, respectively. Using bioinformatics methods, it was revealed that a number of pathways, including the 'androgen receptor signaling pathway', 'androgen receptor activity', 'transcription factor binding' and 'protein processing in the endoplasmic reticulum', were important in PCa. A total of seven hub genes, including phosphoribosylaminoimidazole carboxylase and phosphoribosylaminoimidazolesuccin ocarboxamide synthase (PAICS), cadherin 1 (CDH1), SRC proto-oncogene, non-receptor tyrosine kinase, twist family bHLH transcription factor 1 (TWIST1), ZW10 interacting kinetochore protein (ZWINT), PCNA clamp associated factor (KIAA0101) and androgen receptor, among which, five (PAICS, CDH1, TWIST1, ZWINT and KIAA0101) were significantly upregulated and negatively correlated with miR-1, were identified as key miR-1 target genes in PCa. Additionally, it was investigated whether miR-1 and its hub genes were associated with clinical features, including age, tumor status, residual tumor, lymph node metastasis, pathological T stage and prostate specific antigen level. Collectively the results suggest that miR-1 may be involved in the progression of PCa, and consequently be a promising diagnostic marker. The 'androgen receptor signaling pathway', 'androgen receptor activity', 'transcription factor binding' and 'protein processing in the endoplasmic reticulum' may be crucial interactive pathways in PCa. Furthermore, PAICS, CDH1, TWIST1, ZWINT and KIAA0101 may serve as crucial miR-1 target genes in PCa.

Correspondence to: Dr Hai-Biao Yan, Department of Urological Surgery, The First Affiliated Hospital of Guangxi Medical University, 6 Shuangyong Road, Nanning, Guangxi Zhuang Autonomous Region 530021, P.R. China
E-mail: yanhaibiao_gxmuyfy@163.com

Abbreviations: PCa, prostate cancer; PSA, prostate-specific antigen; miRNA/miR, microRNA; GEO, Gene Expression Omnibus; TCGA, The Cancer Genome Atlas; SMD, standard mean deviation; SROC, summary receiver operating characteristic; GO, Gene Ontology; KEGG, Kyoto Encyclopedia of Genes and Genomes; PPI, protein-protein interaction; AUC, area under the curve

Key words: miR-1, PCa, meta-analysis, bioinformatics, target gene, signaling pathway

Introduction

Prostate cancer (PCa) remains the cancer with the highest incidence and third highest cause of cancer-associated mortality in males, with an estimated 161,360 new cases and 26,730 mortalities, according to 2017 statistics (1). A number of factors contribute to the survival of patients with PCa, particularly the disease stage at the time of diagnosis. Therefore, the early detection of PCa may improve clinical treatment and patient prognosis. Various techniques for the diagnosis of PCa have been developed; these include pathological biopsy, the gold standard in diagnosis, and other detection methods, including the prostate-specific antigen (PSA) assay (2-4), positron emission tomography (5), multiparametric magnetic resonance imaging (6,7), and urinary long non-coding RNA and microRNA (miRNA/miR) detection (8,9), which have also been used in clinical diagnosis. Despite progress, PCa still requires further novel diagnostic biomarkers to aid in its diagnosis.

miRNAs are known to have a crucial role in the regulation of tumor suppressor genes and oncogenes, resulting in the regulation of cell proliferation and apoptosis (10). miR-1 has been previously reported to be implicated in various tumors (11). The diagnostic value of miR-1 has been reported

in breast cancer (12), colorectal cancer (13) and prostate recurrence (14). Details of the molecular mechanisms of miR-1 in diverse cancer types have been reported over the years. For example, the HOX transcript antisense RNA-miR-1-cyclin D2 axis was reported to promote thyroid cancer cell growth, invasion and migration (15). miR-1 was revealed to suppress colorectal cancer cell proliferation by inhibiting SMAD3-mediated tumor glycolysis (16). In bladder cancer, miR-1 suppressed cell proliferation, invasion and migration by upregulating secreted frizzled-related protein 1 expression (17). miR-1 was also reported to inhibit breast cancer progression by downregulating K-ras and metastasis associated lung adenocarcinoma transcript 1 (18). Regarding PCa, Chang *et al* (19) identified that the epidermal growth factor receptor was able to boost PCa bone metastasis by downregulating miR-1 and activating twist-related protein 1 (TWIST1). Stope *et al* (20) reported that heat-shock protein β-1 reduced the expression of miR-1, which restored oncogenic pathways in PCa cells.

Despite all the studies regarding miR-1 in PCa, to the best of our knowledge, no study has examined its clinical diagnostic significance via systematic meta-analysis and identified the potential target genes and pathways using bioinformatics methods. Therefore, it was necessary for the present study to conduct systematic meta-analysis and bioinformatics analysis to comprehensively evaluate the diagnostic value of miR-1, and examine the potential molecular modulatory mechanisms in PCa. The aim of the present study was to elucidate the diagnostic value of miR-1 in PCa in a more comprehensive way and pose a perspective into the potential molecular mechanism, which may contribute to clinical diagnosis and treatment.

In the present study, a meta-analysis using Gene Expression Omnibus (GEO), The Cancer Genome Atlas (TCGA), ArrayExpress and data from published literature was conducted, to assess the clinical diagnostic value of miR-1 in PCa. By collecting the potential target genes of miR-1 and using bioinformatics analysis, the important targets and signaling pathways of miR-1 in PCa were identified. The present study may aid validation of the diagnostic value of miR-1 in PCa and provide insight into the theoretical molecular modulatory mechanisms for future studies.

Materials and methods

Collection of miR-1 expression data from TCGA. miRNA expression matrix was downloaded from TCGA (https://cancergenome.nih.gov/) (21). The expression data of miR-1-1 and miR-1-2 were included in the investigation. Samples missing miR-1-1 or miR-1-2 expression data were removed from the present research. All the data was normalized using log2 conversion. Additionally, mRNA data was downloaded from the portal of prostate adenocarcinoma in TCGA. The DESeq package (22) in the R program (version 3.30) was applied to obtain the differentially expressed genes (DEGs).

Retrieval of GEO and ArrayExpress PCa datasets. To analyze the expression level of miR-1 in PCa and non-tumor tissue, the GEO and ArrayExpress databases were searched. The key words were as follows: Prostat* and (malignan* OR cancer OR tumor OR tumour OR tumor OR neoplas* OR carcinoma). Microarray datasets that contained the miR-1 values were included. All the data in the datasets were calculated in the log2 scale for normalization. To collect DEGs in PCa following miR-1 pretreatment, the Gene Expression Omnibus (GEO) and ArrayExpress databases were additionally searched with the following retrieval strategies: Prostat* and (malignan* OR cancer OR tumor OR tumor OR neoplas* OR carcinoma) and (miR-1 OR miRNA-1 OR microRNA-1 OR miR1 OR miRNA1 OR microRNA1 OR 'miR 1' OR 'miRNA 1' OR 'microRNA 1' OR miR-1-3p OR miRNA-1-3p OR microRNA-1-3p OR miR-1-1 OR miR-1-2 OR miR1-1 OR miR1-2). Microarrays containing mRNA expression following miR-1 silencing or overexpression were enrolled for further analysis.

Retrieval of published literatures. PubMed (https://www.ncbi.nlm.nih.gov/pubmed/), Science Direct (https://www.sciencedirect.com/), Google Scholar (https://scholar.google.com/), Ovid (http://www.ovid.com), Wiley Online Library (https://onlinelibrary.wiley.com/), EMBASE (https://www.embase.com), Web of Science (https://clarivate.com/products/web-of-science/), Chong Qing VIP (http://qikan.cqvip.com/), CNKI (http://cnki.net/), Wan Fang (www.wanfangdata.com.cn) and China Biology Medicine Disc (http://www.sinomed.ac.cn/) were used for literature retrieval. The searching strategies were as follows: Prostat* and (malignan* OR cancer OR tumor OR tumor OR neoplas* OR carcinoma) and (miR-1 OR miRNA-1 OR microRNA-1 OR miR1 OR miRNA1 OR microRNA1 OR 'miR 1' OR 'miRNA 1' OR 'microRNA 1' OR miR-1-3p OR miRNA-1-3p OR microRNA-1-3p OR miR-1-1 OR miR-1-2 OR miR1-1 OR miR1-2). Studies for which the mean, standard deviation and case number of miR-1 in prostate cancer and non-tumor groups were available were further analyzed. Additionally, studies that provided the true positive, false positive, false negative and true negative values were included in the diagnostic meta-analysis.

Identification of putative miR-1 target genes. For the microarray data with silenced or overexpressed miR-1, the mRNA expression was analyzed and log2 fold change (FC) was calculated to select the DEGs. $Log_2FC<0$ or $log_2FC>0$ was adopted to screen the downregulated or upregulated genes in the miR-1 overexpressed or silenced microarrays, respectively. Additionally, DEGs were obtained from the TCGA data through the standard $log_2FC>1$. Furthermore, the miRWalk 2.0 tool (http://zmf.umm.uni-heidelberg.de/mirwalk2/) (23), which links to 11 other online prediction databases, was used to predict the putative target genes of miR-1. Targets predicted by more than two datasets were finally selected. Genes that were included as DEGs from the GEO microarrays and TCGA, and the predicted target genes, were filtered further to collect the more specific target genes of miR-1. Finally, the validated target genes reported in the published literature were included in the genes for further analysis.

Bioinformatics analysis. To uncover the potential crucial signal pathways and target genes of miR-1 in PCa, Gene Ontology (GO) annotation and Kyoto Encyclopedia of Genes

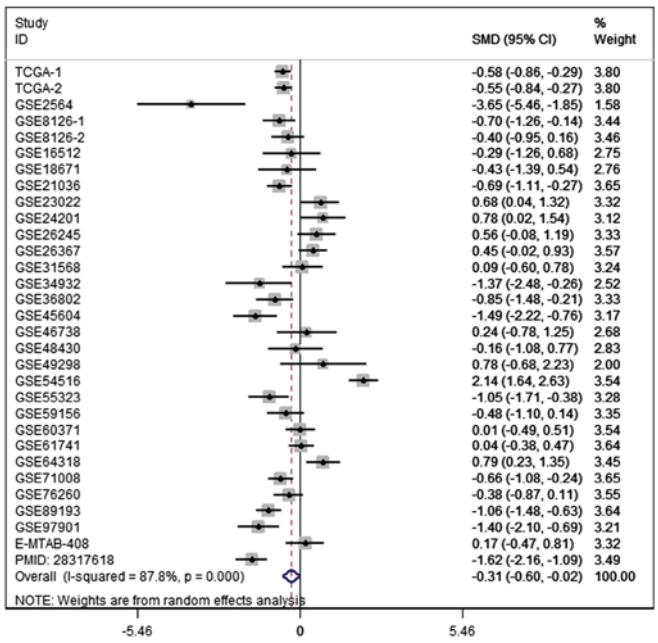

Figure 1. Forest plot of the included data evaluating the expression difference between prostate cancer and normal tissues. Pooled SMD was calculated to present expression difference of miR-1. Random effect model was adopted. SMD, standard mean deviation; CI, confidence intervals; PMID, PubMed ID; TCGA, The Cancer Genome Atlas.

and Genomes (KEGG) pathway analysis were performed using DAVID 6.8 (david-d.ncifcrf.gov/). P<0.05 was considered to indicate a statistically significant difference. The false discovery rate was adopted to reflect the rate of type I errors in multiple comparisons. A protein-protein interaction (PPI) network was plotted using the plugin stringAPP 1.10 in Cytoscape 3.50 (http://www.cytoscape.org/) (24), which has the ability to import the network from the STRING (string-db.org) database. Connection degrees >3 among the nodes were used to select the hub genes.

Validation of the hub genes. GEPIA (gepia.cancer-pku.cn), a newly developed interactive web server, was designed to analyze the RNA sequencing expression data of 9,736 tumors and 8,587 normal samples from the TCGA and the GTEx projects using a standard processing pipeline (25). Thus, GEPIA was used to validate the expression of the hub genes that were selected in the PPI. As miR-1 exerts it functions by specifically binding to its target genes, a Spearman's correlation analysis was conducted to validate the correlation between miR-1 and hub genes. The expression data of miR-1 and hub genes was downloaded from TCGA database. The expression data of miR-1 in TCGA included miR-1-1 and miR-1-2; therefore, the average expression of miR-1-1 and miR-1-2 was calculated to represent the expression of miR-1. The expression data of miR-1 and hub genes were normalized with log2 (x+1).

Clinical value of miR-1 and hub genes in PCa. The data of miR-1, hub genes and clinical phenotype of PCa were obtained from TCGA database. The information of age, cancer status, residual tumor, Tumor, Node, Metastasis stage, survival time, final status, PSA level, hormone therapy and drug response were collected. The expression of miR-1, hub genes and PSA value were normalized with $\log_2$ (x+1). The expression difference analysis of miR-1, phosphoribosylaminoimidazole carboxylase and phosphoribosylaminoimidazolesuccinocarboxamide synthase (PAICS), cadherin 1 (CDH1), SRC proto-oncogene, non-receptor tyrosine kinase (SRC), twist family bHLH transcription factor 1 (TWIST1), ZW10 interacting kinetochore protein (ZW10), ZWINT, PCNA clamp associated factor (KIAA0101) and androgen receptor (AR) among AR-dependent, castrate-resistant (AR-independent) PCa and normal tissues were performed. The correlation among miR-1, upregulated hub genes (PAICS, CDH1, TWIST1, ZWINT and KIAA0101) and PSA was investigated. The association between miR-1, upregulated hub genes (PAICS, CDH1, TWIST1, ZWINT and KIAA0101) and clinicopathological parameters was investigated using SPSS 23.0 (IBM Corp., Armonk, NY, USA).

Statistical analysis. The standard mean deviation (SMD) was used to evaluate the miR-1 expression differences between PCa and adjacent normal tissues via continuous variable meta-analysis in Stata 14.0 (StataCorp LLC, College Station, TX, USA). The fixed effects model was adopted to analyze the SMD if there was no heterogeneity among the included studies (I^2>50; P<0.05). Otherwise, the random effects model was used. Begg and Deeks funnel plots were applied to test the publication bias of the included studies. Additionally, a sensitivity analysis was performed to demonstrate the influence of individual studies on the whole dataset. Summary receiver operating characteristic (SROC) curves, Fagan plots and forest plots of sensitivity, specificity, positive likelihood ratios, negative likelihood ratios, diagnostic scores, in addition to odds ratios depicted through Stata 14.0 (StataCorp LLC), were performed to comprehensively evaluate the diagnostic value of miR-1 in PCa. Furthermore, bivariate boxplots and likelihood matrices were plotted to illustrate the sensitivity, specificity, positive likelihood ratio and negative likelihood ratio in a plane coordinate system. SPSS 23.0 (IBM Corp.) and GraphPad Prism 6 (GraphPad Software, Inc., La Jolla, CA, USA) were used for the clinicopathological parameter analysis and to display the results, respectively. Spearman's correlation analysis was used to analyze the correlation among miR-1, hub genes and PSA level. Student's t test was applied for comparison of two groups and the log-rank test was used for the survival analysis. P<0.05 was considered to indicate a statistically significant difference.

Results

Expression level of miR-1 in PCa. For all the included studies, the combined SMD was -0.31 [95% confidence interval (CI), -0.60 to 0.22] based on the random effects model (I^2=87.8%; Fig. 1). Publication bias was not observed in the funnel plots, as it was basically symmetrical (Fig. 2). Significant heterogeneity was observed in the forest plot. As a result, a sensitivity analysis was performed, and it was considered that GSE54516 may cause heterogeneity (Fig. 3). Following removal of GSE54516, the combined SMD was

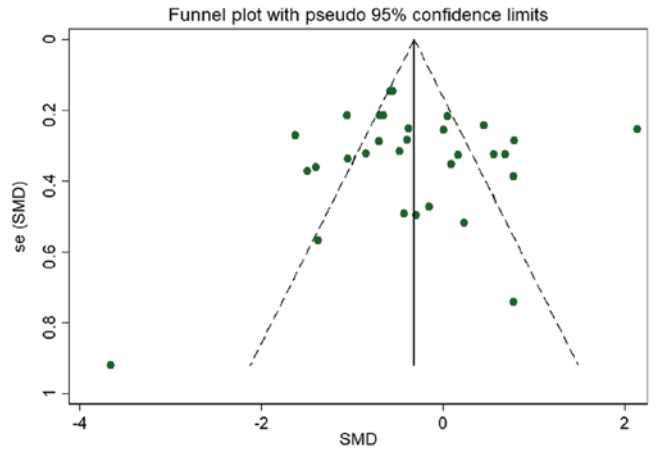

Figure 2. Funnel plot evaluating the publication bias. Each green node represents a separate study. Vertical line represents pooled SMD, while dotted lines represent confident interval. SMD, standard mean deviation; se, standard error.

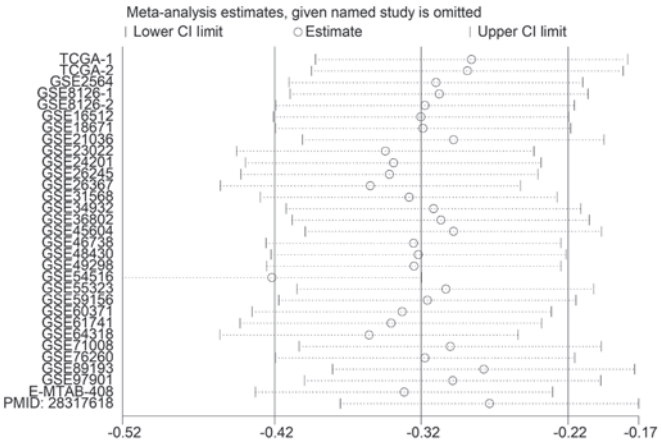

Figure 3. Sensitivity analysis screening the studies that might cause bias. Each study was omitted in turn to seek the source of heterogeneity. CI, confidence interval; PMID, PubMed ID; TCGA, The Cancer Genome Atlas.

-0.42 (95% CI, -0.52 to -0.32) with an I^2=80.4%, which indicated downregulation (Fig. 4).

Diagnostic value of miR-1 in PCa. An SROC curve was used to evaluate the pooled diagnostic value of miR-1 in the included studies. The SROC curve demonstrated that the pooled area under the curve (AUC) was 0.73 (95% CI, 0.69 to 0.77; Fig. 5), which suggested a moderate diagnostic efficacy of miR-1 in PCa. The combined sensitivity and specificity were 0.77 (95% CI, 0.62 to 0.88) and 0.57 (95% CI, 0.41 to 0.72), respectively (Fig. 6). The positive diagnostic likelihood ratio (DLR) and negative DLR were 1.82 (95% CI, 1.36 to 2.43) and 0.40 (95% CI, 0.26 to 0.60), respectively (Fig. 7). The diagnostic score and odds ratios were also calculated and were 1.53 (95% CI, 0.97 to 2.08) and 4.60 (95% CI, 2.63 to 8.04), respectively (Fig. 8). A Fagan plot was used to demonstrate how much the result on the diagnostic test alters the probability that a patient has PCa. The positive and negative posterior probabilities were 31 and 9%, respectively, and the pre-test probability was 20%. (Fig. 9). Deek's funnel plot was created to check

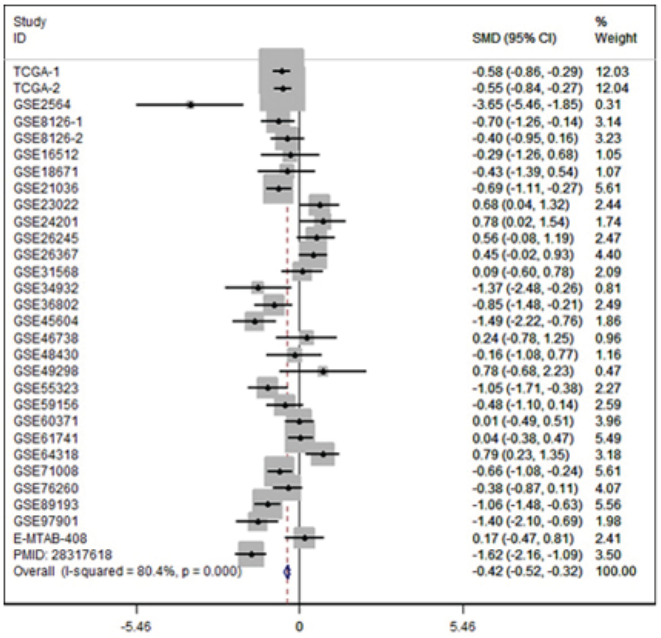

Figure 4. Forest plot evaluating the miR-1 expression difference between prostate cancer and normal tissues after omitting the studies contributing to bias. Pooled SMD was calculated to present expression difference of miR-1. Fixed effect model was adopted. miR, microRNA; SMD, standard mean deviation; CI, confidence interval; PMID, PubMed ID; TCGA, The Cancer Genome Atlas.

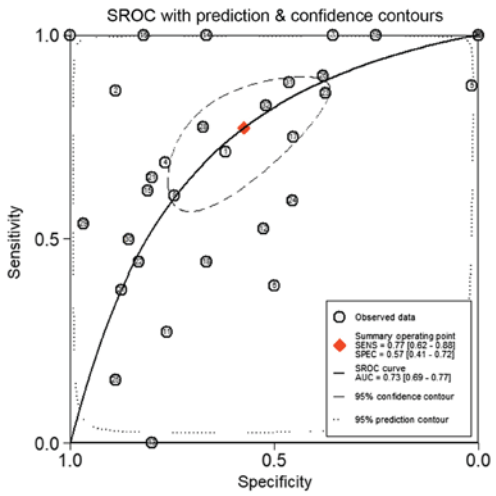

Figure 5. SROC curve evaluating the diagnostic value of miR-1 in prostate cancer. Each plot with Arabic numeral inside represents a separate study. Red diamond represents summary operating point. SROC, summary receiver operating characteristic; AUC, area under the curve; SENS, sensitivity; SPEC, specificity.

for the potential publication bias of included studies. As demonstrated in Fig. 10, the Deek's funnel plot obtained a P-value of 0.85, which suggested there was no publication bias in the diagnostic meta-analysis. A bivariate boxplot was additionally constructed to assess distributional properties of sensitivity vs. specificity and to identify potential outliers (Fig. 11). An index test was used to display informativeness of measured test, which displayed the distribution of positive and negative likelihood ratio in the diagnostic meta-analysis (Fig. 12). Collectively, no publication bias

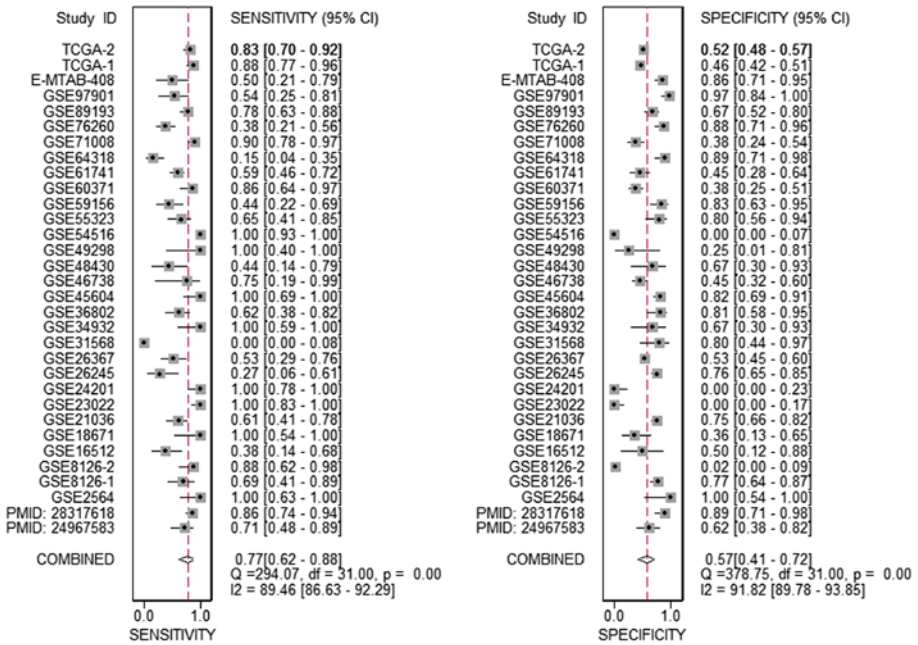

Figure 6. Sensitivity and Specificity Forest plots. Vertical dotted lines represent combined sensitivity and specificity. CI, confidence interval; PMID, PubMed ID; TCGA, The Cancer Genome Atlas.

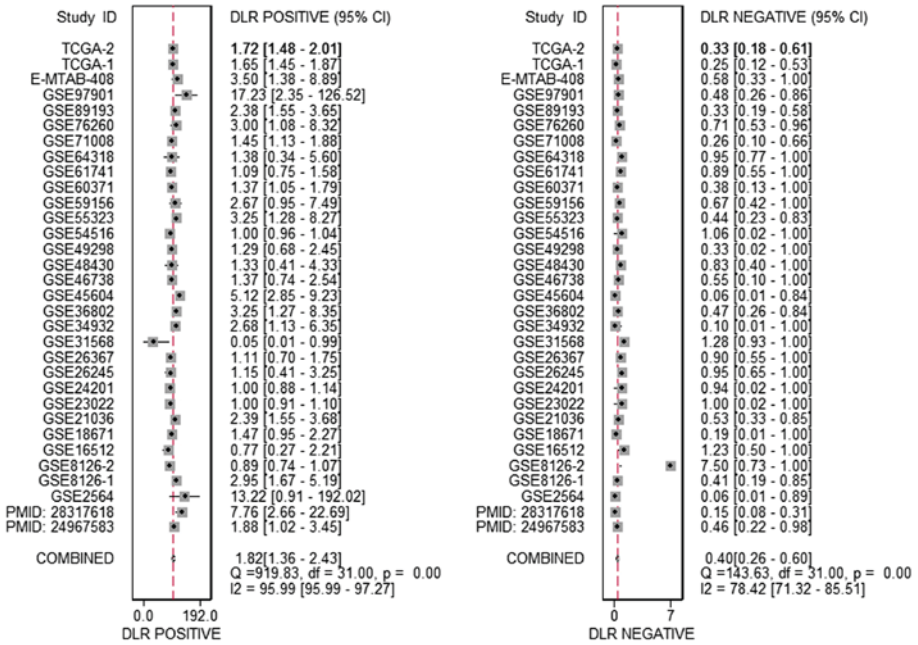

Figure 7. Positive likelihood ratio and negative likelihood ratio forest plots. Vertical dotted lines represent combined positive likelihood and negative likelihood. DLR, diagnostic likelihood ratio; CI, confidence interval; PMID, PubMed ID; TCGA, The Cancer Genome Atlas.

existed in the present study and downregulated miR-1 demonstrated moderate diagnostic accuracy in PCa.

Collection of possible target genes. In the GEO microarray datasets, GSE26032 and GSE31620, which included transfection of pre-miR oligos in prostate carcinoma cell lines to overexpress, were finally included. The expression data of the genes was extracted and the $\log_2$FC was calculated. With the standard $\log_2$FC<0, the downregulated genes were collected. A total of 1,239 genes were finally gathered following intersecting the downregulated genes in GSE26032 and GSE31620, which contained two and three paired samples, respectively. For TCGA DEGs, the $\log_2$FC>1 was restricted and 684 genes were obtained. Furthermore, 10,025 predicted target genes were gathered using the 12 online prediction tools. To improve the specificity of the putative target genes of miR-1, the GEO downregulated genes were intersected, TCGA DEGs, in addition to the predicted genes, and 45 putative significant genes were finally obtained for further bioinformatics analysis (Table I).

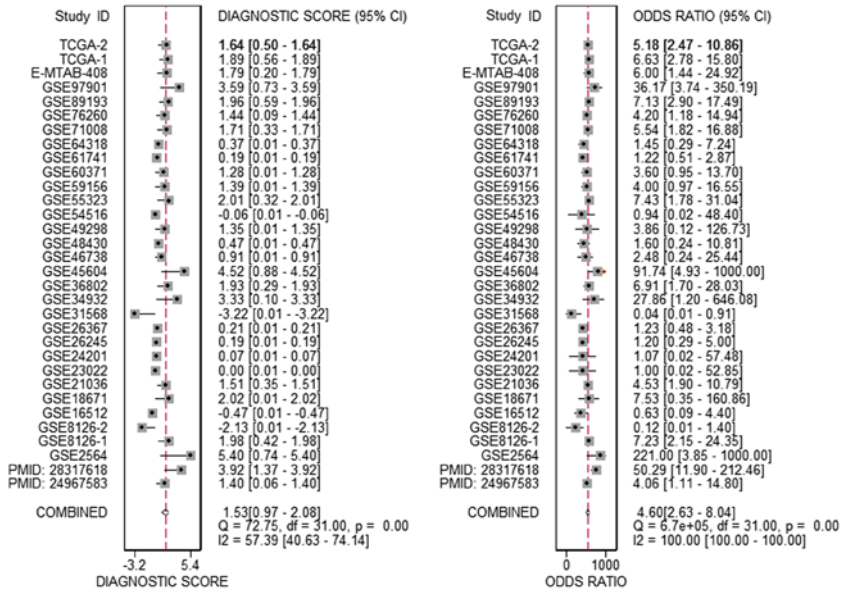

Figure 8. Diagnostic score and odds ratio forest plots. Vertical dotted lines represent diagnostic score and odd ratio. CI, confidence interval; PMID, PubMed ID; TCGA, The Cancer Genome Atlas.

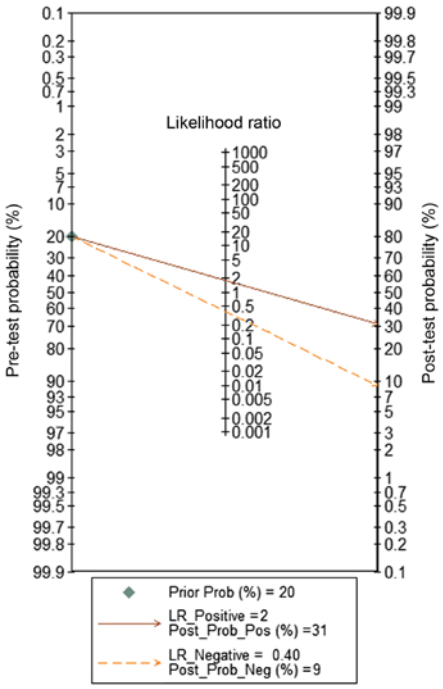

Figure 9. Fagan plot presenting the relationship of prior probability, the likelihood ratio and posterior test probability. The positive and negative likelihood ratio was 2 and 0.4, respectively. LR, likelihood ratio; Prob, probability.

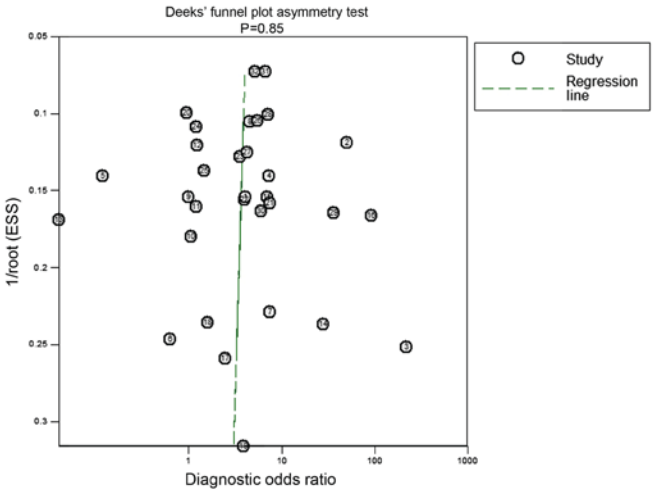

Figure 10. Deek's funnel plot evaluating the publication bias of the included studies in the diagnostic value assessment. P>0.05 was used to determine no publication bias in the investigation. ESS, effective sample size.

Bioinformatics analysis. A total of 45 promising overlapping target genes were collected for the bioinformatics analysis (Table II; Fig. 13). The GO annotation elucidated that the promising target genes of miR-1 were closely associated with 'the response to the drug', 'adherens junction organization' and 'androgen receptor signaling pathway' in the 'biological process' (BP) domain. For the 'cellular component' (CC) domain, the promising miR-1 targets were mostly associated with the 'perinuclear region of cytoplasm', 'extracellular exosome' and 'membrane'. In the 'molecular function' (MF) domain, the putative miR-1 targets were mostly enriched in the 'androgen receptor activity', the 'transcription factor binding' and 'cadherin binding involved in cell-cell adhesion'. In addition, the KEGG pathway analysis demonstrated that the 'protein processing pathway in the endoplasmic reticulum' was the most significant. Using the PPI network, the construction of seven hub genes (PAICS, CDH1, SRC, TWIST1, ZWINT, KIAA0101 and AR) were identified to act as the potential key targets of miR-1 in PCa (Fig. 14).

Validation of the hub genes. The expression of the seven hub genes (PAICS, CDH1, SRC, TWIST1, ZWINT, KIAA0101 and AR) was analyzed in the PCa and adjacent normal samples from TCGA and GTEx. A total of 492 PCa and 152 normal tissue samples were enrolled in the expression validation. Among the seven hub genes, it was observed that five of

Table I. 54 putative potential targets of microRNA-1.

Gene symbol	Official name
SEL1L3	SEL1L family member 3
PPM1H	Protein phosphatase, Mg2+/Mn2+ dependent 1H
LMNB1	Lamin B1
NKX3-1	NK3 homeobox 1
SLC4A4	Solute carrier family 4 member 4
AP1S1	Adaptor related protein complex 1 subunit sigma 1
PPIB	Peptidylprolyl isomerase B
PSAT1	Phosphoserine aminotransferase 1
PABPC1	Poly(A) binding protein cytoplasmic 1
BCAM	Basal cell adhesion molecule (Lutheran blood group)
AGA	Aspartylglucosaminidase
TMEM97	Transmembrane protein 97
SSR1	Signal sequence receptor subunit 1
GALNT1	Polypeptide N-acetylgalacto-saminyltransferase 1
SEC23B	Sec23 homolog B, coat complex II component
GOLM1	Golgi membrane protein 1
DSG2	Desmoglein 2
APLP2	Amyloid β (A4) precursor-like protein 2
GCNT1	Glucosaminyl (N-acetyl) transferase 1, core 2
EPB41L4B	Erythrocyte membrane protein band 4.1 like 4B
CLCN3	Chloride voltage-gated channel 3
PDIA6	Protein disulfide isomerase family A member 6
SLC27A2	Solute carrier family 27 member 2
MYO6	Myosin VI
DSC2	Desmocollin 2
ABCC4	ATP binding cassette subfamily C member 4
SLC45A2	Solute carrier family 45 member 2
NUP210	Nucleoporin 210
PAICS	Phosphoribosylaminoimidazole carboxylase and phosphoribo-sylaminoimidazolesuccino-carboxamide synthase
CENPF	Centromere protein F
ACSL3	Acyl-CoA synthetase long chain family member 3
PPP3CA	Protein phosphatase 3 catalytic subunit α
ABHD2	Abhydrolase domain containing 2
NCAPD3	Non-SMC condensin II complex subunit D3
SEL1L3	SEL1L family member 3
MAP7	Microtubule associated protein 7
ZWINT	ZW10 interacting kinetochore protein
NAAA	N-acylethanolamine acid amidase
TUSC3	Tumor suppressor candidate 3
PCLAF	PCNA clamp associated factor
ETO2	Neuropilin and tolloid like 2
TPD52	Tumor protein D52
CDH1	Cadherin 1
CADM1	Cell adhesion molecule 1
EIF2AK1	Eukaryotic translation initiation factor 2 α kinase 1
PMEPA1	Prostate transmembrane protein, androgen induced 1
PNP	Purine nucleoside phosphorylase
PTMA	Prothymosin α
AR	Androgen receptor
SRC	SRC proto-oncogene, non-receptor tyrosine kinase
TWIST1	Twist family bHLH transcription factor 1
Slug	Snail family transcriptional repressor 2
KLF4	Kruppel like factor 4
XPO6	Exportin 6
TWF1	Twinfilin actin binding protein 1

Table I. Continued.

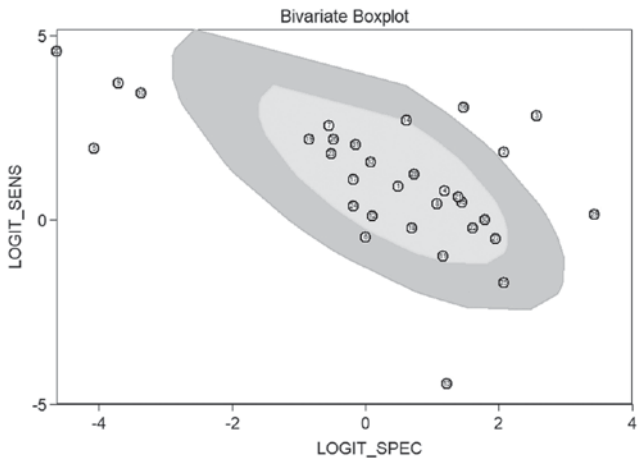

Figure 11. Bivariate boxplot evaluating the sensitivity and specificity in a plane coordinate system. Logit transforms of sensitivity and specificity was used to assess distributional properties of sensitivity vs. specificity and to identify possible outliers. The mean logit sensitivity and specificity with their standard errors and 95% confidence intervals is presented in the gray area. SENS, sensitivity; SPECS, specificity.

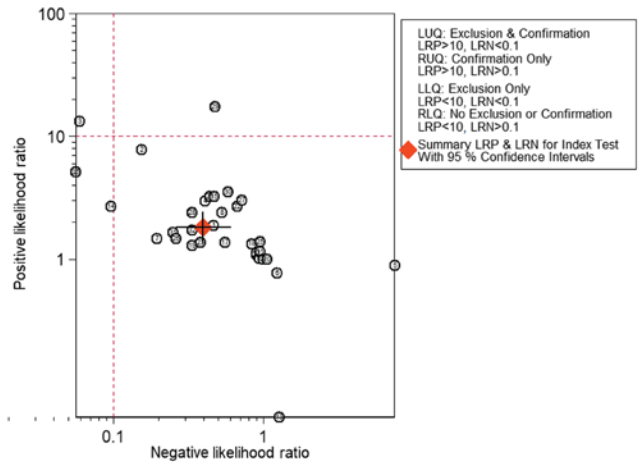

Figure 12. Likelihood matrix evaluating the positive likelihood ratio and negative likelihood ratio in a plane coordinate system. Plot was divided into quadrants based on strength-of-evidence thresholds. Informativeness of measured test was used to determine the distribution of positive and negative likelihood ratio in our diagnostic meta-analysis. LUQ, left upper quadrant; RUQ, right upper quadrant; LLQ, left lower quadrant; RLQ, right lower quadrant; LRP, positive likelihood ratio; LRN, negative likelihood ratio.

Table II. Significant GO and KEGG pathways of the overlapping genes.

Category	Term	Count	P-value	FDR
GOTERM_BP_DIRECT	GO:0042493~response to drug	6	0.00187	2.677129
GOTERM_BP_DIRECT	GO:0034332~adherens junction organization	3	0.005205	7.287529
GOTERM_BP_DIRECT	GO:0030521~androgen receptor signaling pathway	3	0.006361	8.837711
GOTERM_BP_DIRECT	GO:0010628~positive regulation of gene expression	5	0.007078	9.786328
GOTERM_BP_DIRECT	GO:0007156~homophilic cell adhesion via plasma membrane adhesion molecules	4	0.010974	14.78529
GOTERM_BP_DIRECT	GO:0086073~bundle of His cell-Purkinje myocyte adhesion involved in cell communication	2	0.017384	22.45141
GOTERM_BP_DIRECT	GO:0044539~long-chain fatty acid import	2	0.020252	25.66973
GOTERM_BP_DIRECT	GO:0014067~negative regulation of phosphatidylinositol 3-kinase signaling	2	0.028808	34.54625
GOTERM_BP_DIRECT	GO:0006886~intracellular protein transport	4	0.031444	37.07541
GOTERM_BP_DIRECT	GO:0098911~regulation of ventricular cardiac muscle cell action potential	2	0.031644	37.26326
GOTERM_BP_DIRECT	GO:0071456~cellular response to hypoxia	3	0.031963	37.56294
GOTERM_BP_DIRECT	GO:2000679~positive regulation of transcription regulatory region DNA binding	2	0.042905	47.05066
GOTERM_CC_DIRECT	GO:0048471~perinuclear region of cytoplasm	12	9.07E-07	0.001083
GOTERM_CC_DIRECT	GO:0070062~extracellular exosome	21	3.29E-05	0.039319
GOTERM_CC_DIRECT	GO:0016020~membrane	17	0.000218	0.25958
GOTERM_CC_DIRECT	GO:0005913~cell-cell adherens junction	7	0.000272	0.324715
GOTERM_CC_DIRECT	GO:0005789~endoplasmic reticulum membrane	8	0.009743	11.03435
GOTERM_CC_DIRECT	GO:0016323~basolateral plasma membrane	4	0.013947	15.44149
GOTERM_CC_DIRECT	GO:0032587~ruffle membrane	3	0.022114	23.43573
GOTERM_CC_DIRECT	GO:0000139~Golgi membrane	6	0.024307	25.46094
GOTERM_CC_DIRECT	GO:0031965~nuclear membrane	4	0.02621	27.17933
GOTERM_CC_DIRECT	GO:0005783~endoplasmic reticulum	7	0.027342	28.18388
GOTERM_CC_DIRECT	GO:0034663~endoplasmic reticulum chaperone complex	2	0.030365	30.80375
GOTERM_CC_DIRECT	GO:0005794~Golgi apparatus	7	0.032588	32.67453
GOTERM_CC_DIRECT	GO:0016021~integral component of membrane	22	0.032972	32.99373
GOTERM_CC_DIRECT	GO:0005737~cytoplasm	22	0.037093	36.3252
GOTERM_MF_DIRECT	GO:0004882~androgen receptor activity	2	0.009037	12.08615
GOTERM_MF_DIRECT	GO:0008134~transcription factor binding	5	0.010545	12.91881
GOTERM_MF_DIRECT	GO:0098641~cadherin binding involved in cell-cell adhesion	5	0.01132	16.85447
GOTERM_MF_DIRECT	GO:0050839~cell adhesion molecule binding	3	0.015076	19.38597
GOTERM_MF_DIRECT	GO:0008022~protein C-terminus binding	4	0.017579	19.79801
GOTERM_MF_DIRECT	GO:0086083~cell adhesive protein binding involved in bundle of His cell-Purkinje myocyte communication	2	0.017993	23.42536
GOTERM_MF_DIRECT	GO:0005102~receptor binding	5	0.021727	25.48576
GOTERM_MF_DIRECT	GO:0102391~decanoate-CoA ligase activity	2	0.02392	26.92366
GOTERM_MF_DIRECT	GO:0008013~β-catenin binding	3	0.025484	38.00481
GOTERM_MF_DIRECT	GO:0004467~long-chain fatty acid-CoA ligase activity	2	0.038584	57.75621
KEGG_PATHWAY	hsa04141:Protein processing in endoplasmic reticulum	5	0.004469	10.44355

GO, gene ontology; KEGG, Kyoto Encyclopedia of Genes and Genomes; FDR, false discovery rate; BP, biological process; CC, cellular component; MF, molecular function.

them (PAICS, CDH1, KIAA0101, TWIST1, and ZWINT) were significantly upregulated in PCa samples (Fig. 15A-E), which gave them more potential to be the key target genes of miR-1 in PCa. The other two hub genes (SRC and AR) did not demonstrate statistical significance between PCa and normal tissues based on the current data (Fig. 15F and G).

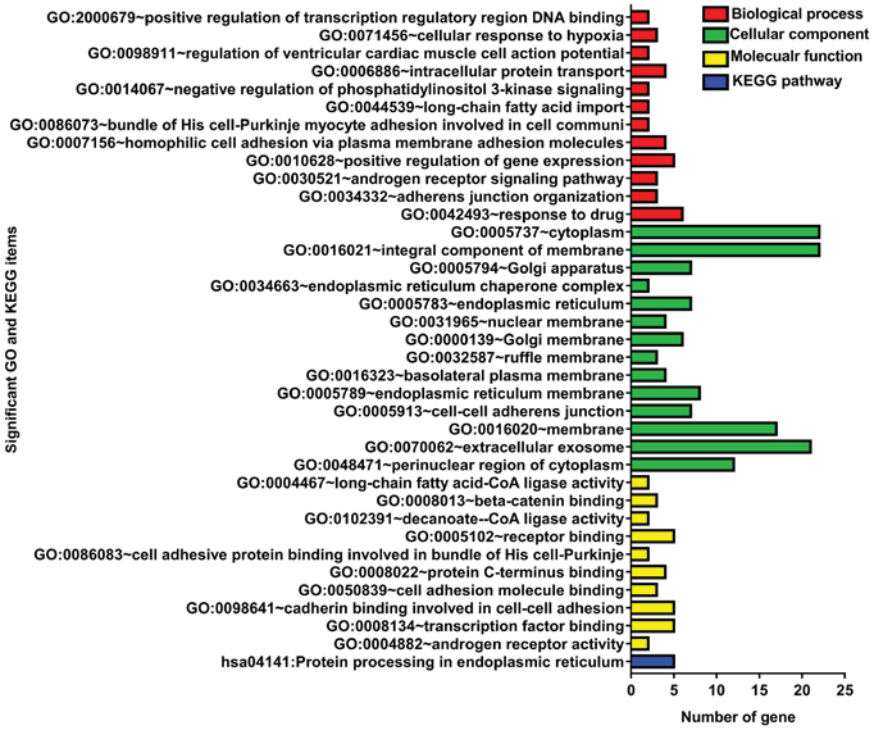

Figure 13. Significant GO annotation and KEGG pathways of the overlapping genes. GO, Gene Ontology; KEGG, Kyoto Encyclopedia of Genes and Genomes.

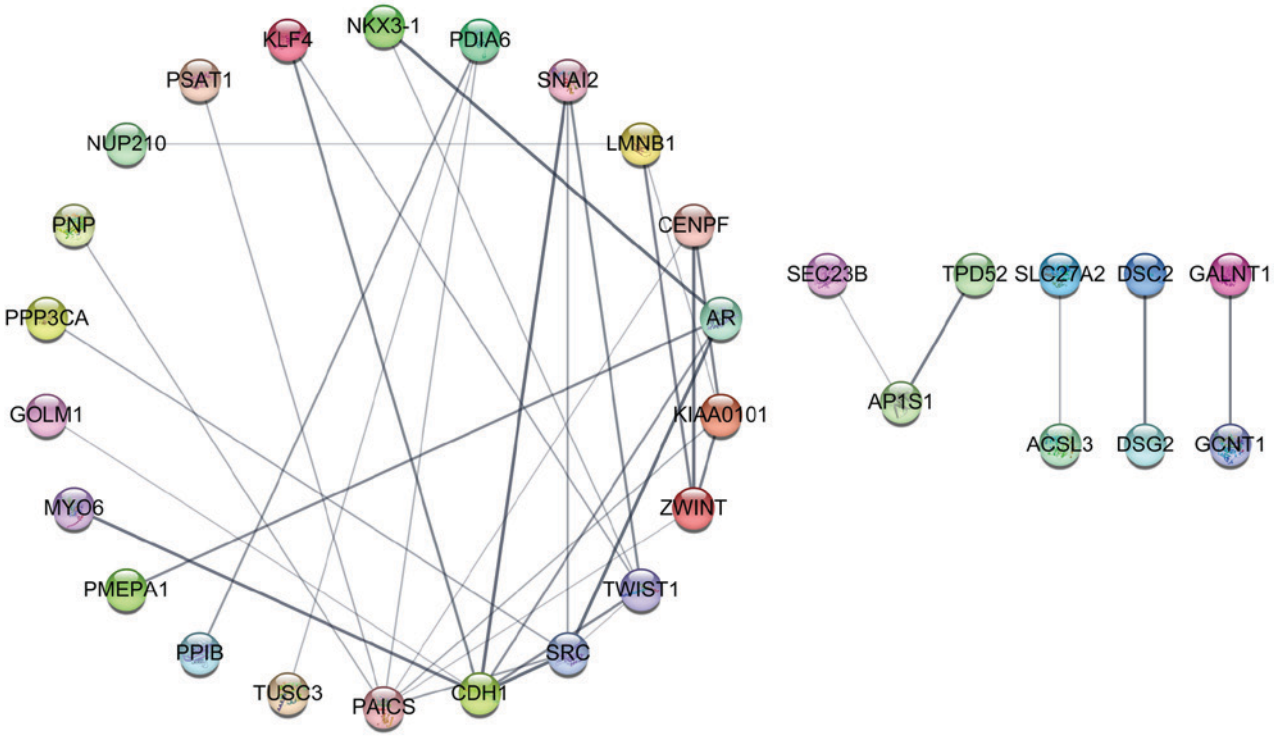

Figure 14. Protein-protein interactive network of the overlapping genes. Each point represents a protein. Degree sorted circle layout was adopted.

Spearman's correlation analysis between miR-1 and the five up-regulated hub genes (PAICS, CDH1, TWIST1, ZWINT and KIAA0101) was performed (Fig. 16). A significant negative correlation was identified between miR-1 and PAICS, ZWINT, in addition to KIAA0101 (P<0.001; Fig. 16A-C), which supported their specific binding. Regarding CDH1 and TWIST1, a trend of negative correlation with miR-1 was observed (Fig. 16D and E). However, no statistical significance was revealed.

Clinical significance of miR-1 and hub genes in PCa. The alterations of miR-1/hub genes among 31 AR-dependent, 9 castrate-resistant PCa and 52 normal tissues were compared. For AR-dependent and castrate-resistant PCa, miR-1 was

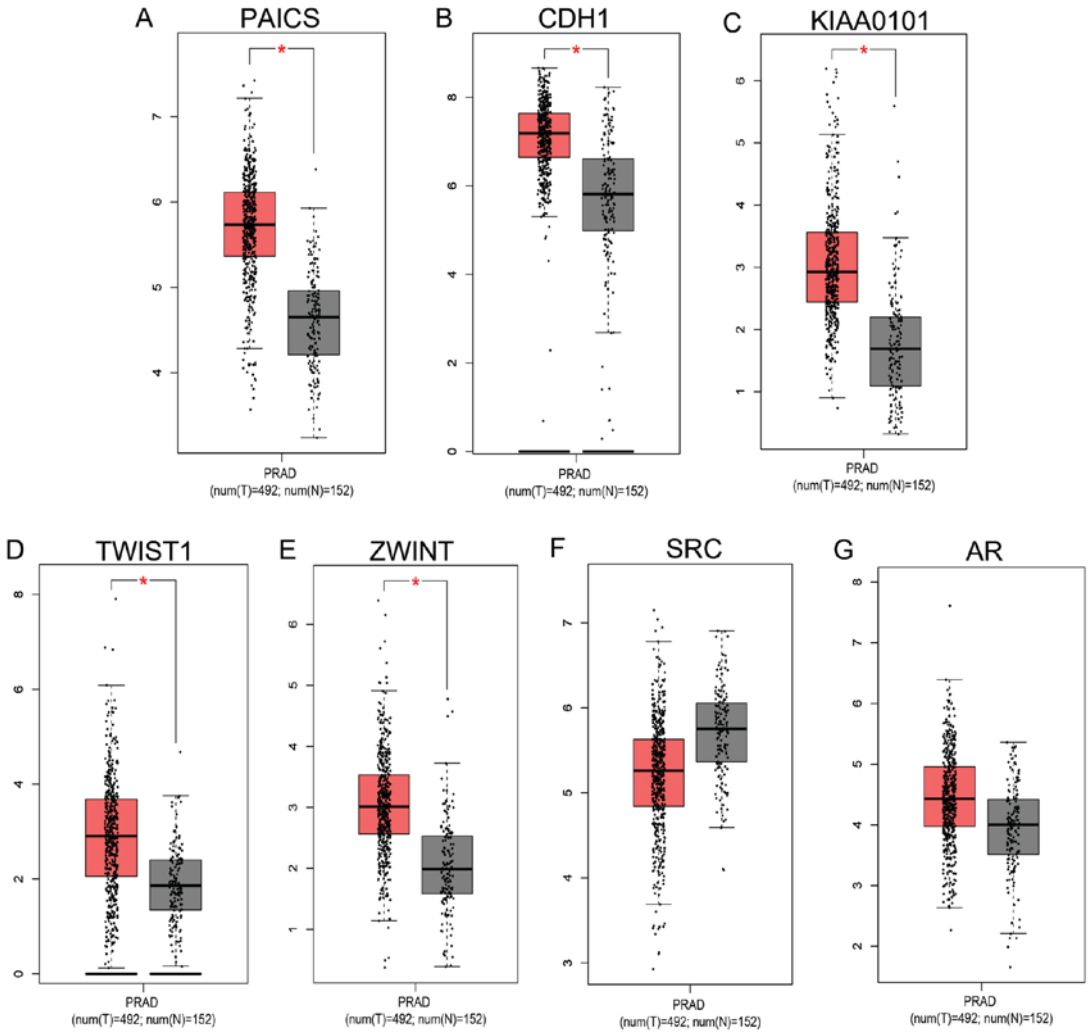

Figure 15. Box plots for the expression of hub genes in prostate cancer and normal tissues. Box plots for the expression of (A) PAICS, (B) CDH1, (C) KIAA0101, (D) TWIST1, (E) ZWINT, (F) SRC and (G) AR. Mean and standard deviation value were calculated for the comparison. *P<0.05. PRAD, prostate adenocarcinoma; PAICS, phosphoribosylaminoimidazole carboxylase and phosphoribosylaminoimidazolesuccino carboxamide synthase; CDH1, cadherin 1; SRC, SRC proto-oncogene, non-receptor tyrosine kinase; TWIST1, twist family bHLH transcription factor 1; ZWINT, ZW10 interacting kinetochore protein; KIAA0101, PCNA clamp associated factor; AR, androgen receptor; T, tumor; N, normal.

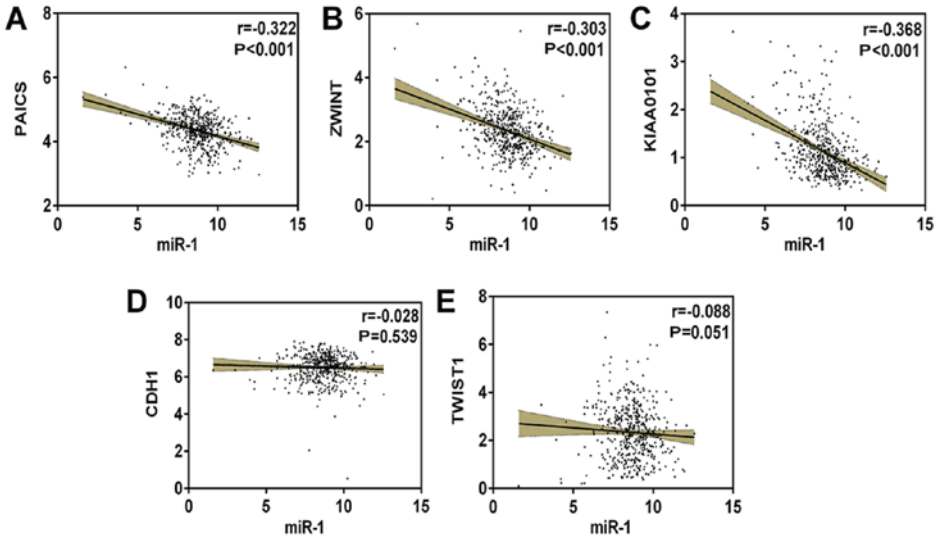

Figure 16. Correlation between miR-1 and its upregulated hub genes. Correlation between miR-1 and (A) PAICS, (B) ZWINT, (C) KIAA0101, (D) CDH1 and (E) TWIST1. Yellow area represents 95% confidence interval. miR, microRNA; PAICS, phosphoribosylaminoimidazole carboxylase and phosphoribosylaminoimidazolesuccinocarboxamide synthase; CDH1, cadherin 1; TWIST1, twist family bHLH transcription factor 1; ZWINT, ZW10 interacting kinetochore protein; KIAA0101, PCNA clamp associated factor.

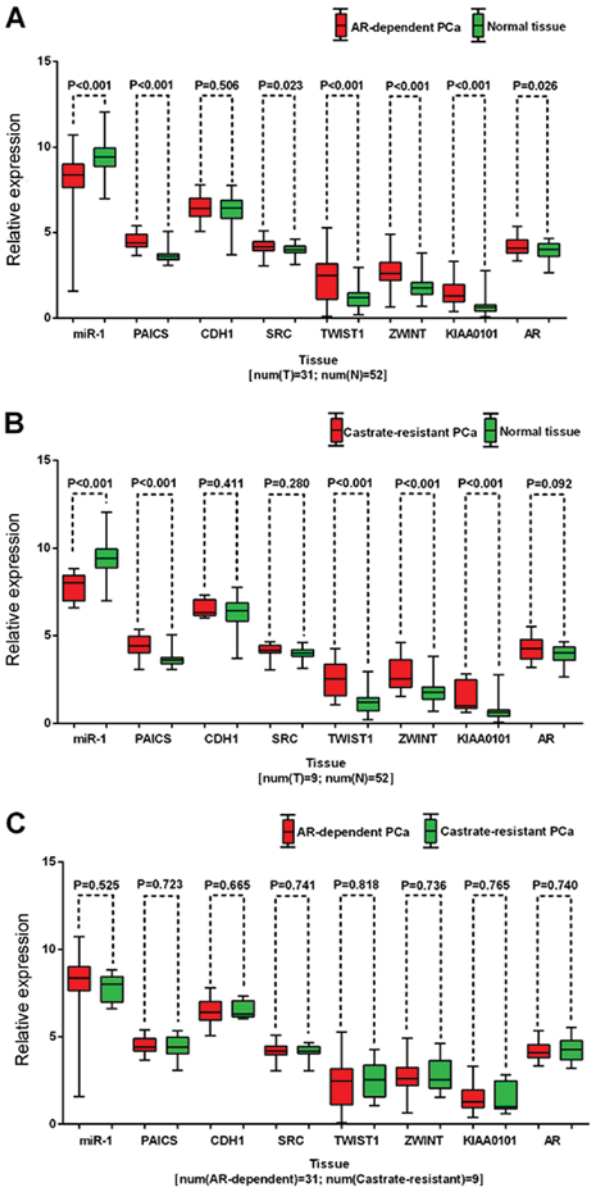

Figure 17. Expression of miR-1 and hub genes among AR-dependent, castrate-resistant PCa and normal tissues. Comparison of miR-1 and hub genes in (A) AR-dependent PCa and normal tissues; (B) castrate-resistant PCa and normal tissues; and (C) AR-dependent PCa and castrate-resistant PCa. Mean and standard deviation value were calculated for the comparison. miR, microRNA; AR, androgen receptor; PCa, prostate cancer; PAICS, phosphoribosylaminoimidazole carboxylase and phosphoribosylaminoimidazolesuccino carboxamide synthase; CDH1, cadherin 1; TWIST1, twist family bHLH transcription factor 1; ZWINT, ZW10 interacting kinetochore protein; KIAA0101, PCNA clamp associated factor.

significantly downregulated; whereas, PAICS, TWIST1, ZWINT and KIAA0101 were significantly upregulated compared with normal tissues (P<0.001; Fig. 17A and B). Regarding CDH1, SRC and AR, the expression of SRC and AR only demonstrated significant increase in AR-dependent PCa not castrate-resistant PCa, while CDH1 did not reveal any alterations in AR-dependent and castrate-resistant PCa compared with normal tissues (Fig. 17A and B). However, for comparison between AR-dependent and castrate-resistant PCa, no statistically significant expression difference of miR-1 or hub genes was observed (Fig. 17C). Further studies with larger samples are required to elucidate the alterations of miR-1 or hub genes among AR-dependent, castrate-resistant PCa and normal tissues. The correlation among miR-1, upregulated hub genes and PSA level was investigated. In Fig. 18, the expression of miR-1 was negatively correlated with PSA level. Regarding the five upregulated hub genes, statistically significant negative correlation among PAICS, ZWINT, KIAA0101 and PSA level was identified. However, for CDH1 and TWIST1, no significantly negative correlation with PSA level was revealed. A total of 491 PCa samples were included for the clinicopathological features analysis. As demonstrated in Table III, the association among miR-1, upregulated hub genes and clinicopathological parameters is presented. In summary, miR-1 was significantly associated with cancer status, distant metastasis and lymph node metastasis and CDH1 was identified to be associated with age, cancer status and residual tumor. TWIST1 was only associated with pathological T stage. Furthermore, ZWINT was associated with cancer status, residual tumor, lymph node metastasis and pathological T stage; whereas, KIAA0101 was associated with age, cancer status, residual tumor, lymph node metastasis and pathological T stage. However, regarding PAICS, no statistically significant association with clinicopathological features was identified, and survival analysis of miR-1 and hub genes did not demonstrate statistical significance (data not shown).

Discussion

PCa is the cancer type that results in the highest worldwide morbidity in the male population (1). Searching for novel diagnostic biomarkers and examining the molecular mechanisms in PCa are of great importance for its clinical diagnosis and treatment. The present study aimed to evaluate the diagnostic value of miR-1 and identify the key target genes and signaling pathways in PCa.

Using comprehensive meta-analysis of expression data from the GEO, ArrayExpress, TCGA and published literature, it was identified that the expression of miR-1 was significantly downregulated in PCa compared with the adjacent normal tissues. It was demonstrated that miR-1 has a moderate diagnostic value in PCa (AUC, 0.73; sensitivity, 0.77; specificity, 0.57; odds ratio, 4.60). To the best of our knowledge, there is only one study, conducted by Pashaei *et al* (26), which has identified downregulated miR-1 in recurrent PCa using a meta-analysis. However, there were only six GEO datasets included in the meta-analysis (26). A larger sample may improve the integration and conviction of the study. In the present study, 27 GEO datasets, two published studies, one ArrayExpress microarray and two sets of TCGA data were analyzed.

Based on the online prediction databases, the potential target genes of miR-1 were collected to further examine the key enriched metabolic pathways in PCa. Subsequently, GO analysis revealed the enriched pathways in three categories. In 'BP', the 'response to drug', 'adherens junction organization', and 'androgen receptor signaling' pathways were the top three pathways. In 'CC', the top three items were the 'perinuclear region of the cytoplasm', the 'extracellular exosome', and the 'membrane'. In the 'MF', the target genes were primarily enriched in 'androgen receptor activity', 'transcription

Table III. Association between miR-1/hub genes and clinicopathological parameters in prostate cancer.

A, miR-1

Clinicopathological feature	n	Expression (mean ± SD)	t-test	P-value
Age (years)			1.605	0.109
<60	199	8.759±1.229		
≥60	292	8.569±1.332		
Tumor status			-2.317	0.021[a]
With tumor	93	8.391±1.328		
Tumor-free	310	8.746±1.286		
Residual tumor			1.836	0.067
No	311	8.728±1.255		
Yes	150	8.495±1.318		
Distant metastasis			-4.455	0.000[a]
No	451	4.617±2.286		
Yes	2	8.677±1.283		
Lymph node metastasis			2.764	0.006[a]
No	342	8.713±1.251		
Yes	77	8.281±1.172		
Pathological T			1.869	0.062
T1 + T2	186	8.782±1.183		
T3 + T4	298	8.561±1.316		

B, PAICS

Clinicopathological feature	n	Expression (mean ± SD)	t-test	P-value
Age (years)			0.48	0.631
<60	199	4.368±0.489		
≥60	292	4.347±0.488		
Tumor status			1.156	0.249
With tumor	93	4.409±0.576		
Tumor-free	310	4.340±0.473		
Residual tumor			-0.153	0.878
No	311	4.358±0.488		
Yes	150	4.365±0.493		
Distant metastasis			1.788	0.075
No	451	4.350±0.486		
Yes	2	4.966±0.697		
Lymph node metastasis			0.213	0.832
No	342	4.356±0.509		
Yes	77	4.343±0.406		
Pathological T			-1.193	0.233
T1 + T2	186	4.323±0.485		
T3 + T4	298	4.377±0.487		

Table III. Continued.

C, CDH1

Clinicopathological feature	n	Expression (mean ± SD)	t-test	P-value
Age (years)			2.4	0.017[a]
<60	199	6.593±0.710		
≥60	292	6.431±0.754		
Tumor status			-3.135	0.002[a]
With tumor	93	6.306±1.018		
Tumor-free	310	6.586±0.658		
Residual tumor			2.967	0.003[a]
No	311	6.583±0.636		
Yes	150	6.338±0.912		
Distant metastasis			-1.192	0.234
No	451	6.490±0.723		
Yes	2	5.880±0.697		
Lymph node metastasis			1.185	0.237
No	342	6.521±0.681		
Yes	77	6.409±1.003		
Pathological T			1.631	0.104
T1+T2	186	6.567±0.646		
T3+T4	298	6.454±0.793		

D, TWIST1

Clinicopathological feature	n	Expression (mean ± SD)	t-test	P-value
Age (years)			-0.549	0.583
<60	199	2.307±1.131		
≥60	292	2.363±1.107		
Tumor status			1.274	0.203
With tumor	93	2.404±1.198		
Tumor-free	310	2.240±1.056		
Residual tumor			-1.636	0.103
No	311	2.271±1.067		
Yes	150	2.454±1.241		
Distant metastasis			1.444	0.150
No	451	2.329±1.110		
Yes	2	3.463±0.032		
Lymph node metastasis			-1.629	0.104
No	342	2.271±1.067		
Yes	77	2.501±1.329		
Pathological T			-2.244	0.025[a]
T1+T2	186	2.200±1.053		
T3+T4	298	2.434±1.154		

Table III. Continued.

E, ZWINT

Clinicopathological feature	n	Expression (mean ± SD)	t-test	P-value
Age (years)			-1.482	0.139
<60	199	2.279±0.693		
≥60	292	2.375±0.715		
Cancer status			3.495	0.001[a]
With tumor	93	2.570±0.839		
Tumor-free	310	2.241±0.645		
Residual tumor			-3.458	0.001[a]
No	311	2.255±0.641		
Yes	150	2.505±0.764		
Distant metastasis			0.629	0.643
No	451	2.339±0.693		
Yes	2	3.629±2.902		
Lymph node metastasis			-3.193	0.002[a]
No	342	2.287±0.662		
Yes	77	2.607±0.821		
Pathological T			-4.94	0.000[a]
T1+T2	186	2.157±0.526		
T3+T4	298	2.445±0.758		

F, KIAA0101

Clinicopathological feature	n	Expression (mean ± SD)	t-test	P-value
Age (years)			-2.284	0.023[a]
<60	199	1.067±0.506		
≥60	292	1.181±0.590		
Cancer status			3.41	0.001[a]
With tumor	93	1.322±0.692		
Tumor-free	310	1.059±0.495		
Residual tumor			-3.188	0.002[a]
No	311	1.063±0.498		
Yes	150	1.249±0.624		
Distant metastasis			0.958	0.514
No	451	1.135±0.553		
Yes	2	2.353±1.799		
Lymph node metastasis			-2.806	0.006[a]
No	342	1.118±0.532		
Yes	77	1.347±0.671		

Table III. Continued.

F, KIAA0101

Clinicopathological feature	n	Expression (mean ± SD)	t-test	P-value
Pathological T			-6.185	0.000[a]
T1+T2	186	0.960±0.405		
T3+T4	298	1.243±0.599		

[a]Statistically significant. miRNA/miR, microRNA; SD, standard deviation; PAICS, phosphoribosylaminoimidazole carboxylase and phosphoribosylaminoimidazolesuccinocarboxamide synthase; CDH1, cadherin 1; TWIST1, twist family bHLH transcription factor 1; ZWINT, ZW10 interacting kinetochore protein; KIAA0101, PCNA clamp associated factor.

factor binding' and 'cadherin binding in cell-cell adhesion'. Furthermore, KEGG analysis identified a significant pathway, namely 'protein processing in the endoplasmic reticulum'. Among the above pathways discovered, it was identified that the 'androgen receptor signaling pathway', 'androgen receptor activity', 'transcription factor binding' and 'protein processing in the endoplasmic reticulum' have been previously reported. The 'androgen receptor signaling pathway' has been implicated in the therapeutic strategies of PCa (27-29). Regarding the 'androgen receptor activity', Ylitalo *et al* (30) documented that it was involved in castrate-resistant PCa bone metastases. The regulation of androgen receptor activity was additionally discovered to be associated with therapy resistance and disease progression in PCa (31-33). Furthermore, transcription factor binding sites were additionally identified to be a crucial reaction domain in PCa, which may aid the explanation of the underlying regulatory mechanism (34,35). Regarding KEGG pathway analysis, Kojima *et al* (36) additionally revealed that 'protein processing in the endoplasmic reticulum' was a significant miR-143/145 regulated signal pathway in PCa, which may provide novel insights into the potential mechanism of PCa oncogenesis and metastasis. In summary, the enriched pathways, namely, the 'androgen receptor signaling pathway', 'androgen receptor activity', 'transcription factor binding', and 'protein processing in the endoplasmic reticulum', possess great potential to be involved the regulatory mechanisms of miR-1 in PCa. For the other pathways that have not been reported in PCa, further examination of their role in the regulatory mechanisms of miR-1 in PCa is worth pursuing.

Using the PPI network, seven hub genes (PAICS, CDH1, SRC, TWIST1, ZWINT, KIAA0101 and AR) that may be the key target genes of miR-1 in PCa were identified. As miR-1 was downregulated in PCa, according to the meta-analysis, it was hypothesized that its target genes are upregulated accordingly. Thus, the expression of five hub genes was validated based on TCGA and GTEx data. It was identified that the five hub genes (PAICS, CDH1, TWIST1, ZWINT and KIAA0101) were significantly upregulated in PCa. Since miR-1 was able to specifically bind to its targets, it was hypothesized that there is a correlation between miR-1 and its targets. As expected, there

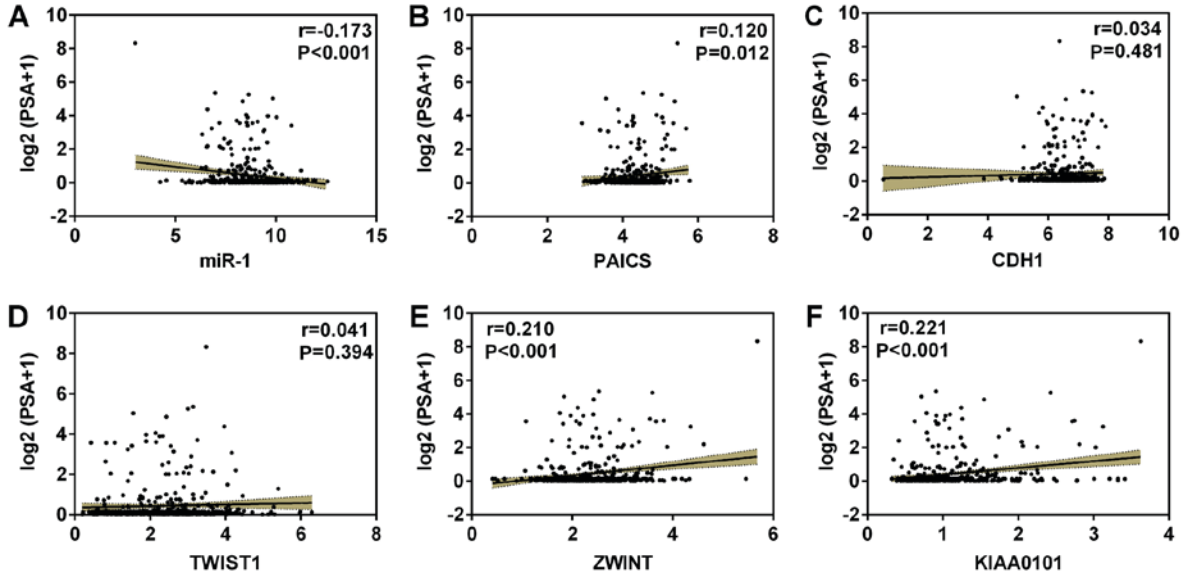

Figure 18. Correlation between miR-1 or hub genes and PSA level. Correlation between PSA level and (A) miR-1, (B) PAICS, (C) CHD1, (D) TWIST1, (E) ZWINT and (F) KIAA0101 Yellow area represents 95% confidence interval. miR, microRNA; PSA, prostate-specific antigen; PAICS, phosphoribosylaminoimidazole carboxylase and phosphoribosylaminoimidazolesuccinocarboxamide synthase; CDH1, cadherin 1; TWIST1, twist family bHLH transcription factor 1; ZWINT, ZW10 interacting kinetochore protein; KIAA0101, PCNA clamp associated factor.

was significant negative correlation between miR-1 expression, and PAICS, ZWINT and KIAA0101 expression. Regarding CDH1 and TWIST1, a there was no significant correlation with miR-1. AR-dependent and castrate-resistant PCa may have different miRNA/mRNA expression profiles. Therefore, the expression of miR-1 and hub genes among AR-dependent, castrate-resistant PCa and normal tissues was investigated. In summary, it was identified that there was a trend that miR-1 was downregulated, while hub genes were upregulated in AR-dependent and castrate-resistant PCa compared with normal tissues. However, the expression difference of miR-1 and hub genes between AR-dependent and castrate-resistant PCa remains unclear. Studies with a larger sample size are required to elucidate the expression profiling alterations of miR-1/hub genes in AR-dependent and castrate-resistant PCa. Considering that PSA level was a useful specific marker in the clinical diagnosis of PCa, the correlation between miR-1/hub genes and PSA level was investigated. Notably, it was identified that miR-1 was negatively correlated with PSA level, while hub genes, PAICS, ZWINT and KIAA0101, were positively correlated with PSA level. Furthermore, it was identified that miR-1 and its hub genes were significantly associated with specific clinical phenotypes including age, tumor status, residual tumor, lymph node metastasis and pathological T stage. These results may pose a perspective for the clinical application of miR-1 and its hub genes. Combining PSA with miR-1/hub genes may be useful for the clinical diagnosis of PCa, and the involved molecular mechanism of miR-1 and its hub genes may shed light on novel therapies for patients with PCa. Consequently, the five upregulated genes, PAICS, CDH1, TWIST1, ZWINT and KIAA0101 were focused on for a more detailed discussion.

PAICS encodes a bifunctional enzyme. The octameric structure of the bifunctional enzyme PAICS in purine biosynthesis may contribute to PAICS-specific inhibitor design, which may be used in cancer chemotherapy (37). PAICS has been reported as a therapeutic target in breast cancer (38). Furthermore, increased PAICS was additionally identified to be associated with poor prognosis in lung cancer, which made it a promising prognostic biomarker (39). Cifola *et al* (40) first identified that PAICS was a mutated gene in melanoma. In the study conducted by Chakravarthi *et al* (41), the role of PAICS in the proliferation and invasion of PCa cell was evaluated, implying that PAICS was a therapeutic target. Collectively, PAICS may be a promising target in PCa. However, its association with miR-1 still requires experimental validation.

CDH1, additionally termed uvomorulin and CDHE, encodes a classical cadherin of the cadherin superfamily. Loss of or reduced expression of CDH1 is thought to contribute to more invasive tumors (42). A previous study discovered that CDH1 polymorphisms may be a prognostic indicator in non-metastatic laryngeal cancer (43). Jiao *et al* (44) identified that aberrant CDH1 was able to predict a poor prognosis for patients with pancreatic cancer. In addition, CDH1 was additionally identified to be associated with the risk of lung cancer (45), breast cancer (46), and gastric cancer (47), and may be a potential drug target. In PCa, there was additionally a meta-analysis that evaluated CDH1-60 C/A polymorphism as a risk factor in the development of PCa (48). In summary, CDH1 was a promising key target in PCa; however, it requires further experimental evaluation.

TWIST1 was reported to be implicated in cell lineage determination and differentiation. TWIST1 has been revealed to serve as an effective target for cancer metastasis and chemoresistance (49). In pancreatic cancer, TWIST1 was identified as a therapeutic target and prognostic marker for tumor metastasis (50). TWIST1 was additionally a target in lung cancer, which was correlated with the inhibition of proliferation, epithelial-mesenchymal transition and metastasis (51). Furthermore, overexpression of TWIST1

was additionally identified to determine lung cancer chemoresistance and prognosis (52). TWIST1 was additionally documented to be associated with the invasion and metastasis of gastric cancer (53,54), and was a potential prognostic marker in colorectal cancer (55-57). Regarding PCa, numerous studies have reported that TWIST1 was involved in progression, including cancer invasion, migration and migration (58-63). As for the association between miR-1 and TWIST1, Chang *et al* (19) discovered that epidermal growth factor receptor translocation promotes the bone metastasis of PCa by downregulating miR-1, which directly increases the expression of TWIST1. Given the above information, TWIST1 may be considered a key target of miR-1 in PCa. This finding requires further experimental research to validate it.

ZWINT encodes a protein that is involved in kinetochore function. Xu *et al* (64) identified that ZWINT was increased in ovarian cancer and correlated with worse overall survival in patients with ovarian cancer. In bladder cancer, Ho *et al* (65) observed that ZWINT was associated with a cell proliferation marker. ZWINT was additionally identified to be significantly correlated with the clinical outcome of chronic lymphocytic leukemia (66). The association between ZWINT and PCa has not been reported in previously published literature. Further evidence is required to further elucidate the function of ZWINT in PCa.

KIAA0101 has been widely reported in the progression of various cancer types. For example, in hepatocellular carcinoma, overexpressed KIAA0101 was significantly associated with distant metastasis, advanced stage, early tumor recurrence and poor prognosis, which made it a potential therapeutic target (67-69). In gastric cancer, KIAA0101 was identified to be involved in the proliferation and invasion of PCa cells (70,71). In addition, overexpression of KIAA0101 was indicated to predict poor survival in lung cancer (72), esophageal cancer (73) and renal cancer (74). As for its role in PCa, to the best of our knowledge, no study at present has elucidated the association between KIAA0101 and PCa. Therefore, further studies are required to determine the precise role of KIAA0101 in PCa.

Collectively, it was identified that miR-1 was downregulated in PCa and was negatively correlated with PSA level. miR-1 was additionally associated with the tumor status, metastasis and lymph node metastasis of PCa. A total of seven hub genes, PAICS, CDH1, SRC, TWIST1, ZWINT, KIAA0101 and AR, were identified. Five of them (PAICS, CDH1, TWIST1, ZWINT and KIAA0101) were significantly upregulated in PCa and were negatively correlated with miR-1, which made them potential key target genes of downregulated miR-1 in PCa. The hub genes were associated with certain clinical features, including age, tumor status, residual tumor, lymph node metastasis, pathological T stage and PSA level. Using a review of published studies, further evidence was provided to support PAICS, CDH1 and TWIST1 as potential target genes of miR-1 in PCa. For ZWINT and KIAA0101, there is a lack of sufficient studies to demonstrate their role in PCa, and as such, they require further exploration. All the analyses in the present study were based on online database sources at the bioinformatics level. Therefore, further experimental studies are required to validate these genes. Nevertheless, the results obtained in the present study may aid the clinical diagnosis of PCa and provide insight into the molecular mechanisms of PCa.

Acknowledgements

Not applicable.

Funding

The present study was funded by the Promoting Project of Basic Capacity for Young and Middle-aged University Teachers in Guangxi (grant no. KY2016LX034). The funders had no role in study design, data collection and analysis, preparation of the manuscript, or decision to publish.

Availability of data and materials

All the data and materials used in the study are currently available at Pubmed (https://www.ncbi.nlm.nih.gov/pubmed/), GEO (https://www.ncbi.nlm.nih.gov/geo/), ArrayExpress (https://www.ebi.ac.uk/arrayexpress/),TCGA(https://cancergenome.nih.gov/), miRWalk 2.0 (http://zmf.umm.uni-heidelberg.de/apps/zmf/mirwalk2/), DAVID (https://david.ncifcrf.gov/) and STRING (https://string-db.org/) databases.

Authors' contributions

HB-Y, SH-L and GC designed the study and revised the manuscript. ZC-X, JC-H, LJ-Z, BL-G and DY-W contributed to the collection and analysis of the data, in addition to the writing of the manuscript.

Ethics approval and consent to participate

Not applicable.

Patient consent for publication

Not applicable.

Competing interests

The authors declare that they have no competing interests.

References

1. Siegel RL, Miller KD and Jemal A: Cancer statistics, 2017. CA Cancer J Clin 67: 7-30, 2017.
2. Lavi A and Cohen M: Prostate cancer early detection using psa-current trends and recent updates. Harefuah 156: 185-188, 2017 (In Hebrew).
3. Filella X and Foj L: Prostate cancer detection and prognosis: From prostate specific antigen (PSA) to exosomal biomarkers. Int J Mol Sci 17: pii: E1784, 2016.
4. Kirby R: The role of PSA in detection and management of prostate cancer. Practitioner 260: 17-21, 3, 2016.
5. Bednarova S, Lindenberg ML, Vinsensia M, Zuiani C, Choyke PL and Turkbey B: Positron emission tomography (PET) in primary prostate cancer staging and risk assessment. Transl Androl Urol 6: 413-423, 2017.
6. Wallis CJD, Haider MA and Nam RK: Role of mpMRI of the prostate in screening for prostate cancer. Transl Androl Urol 6: 464-471, 2017.

7. Johnson DC and Reiter RE: Multi-parametric magnetic resonance imaging as a management decision tool. Transl Androl Urol 6: 472-482, 2017.
8. Balacescu O, Petrut B, Tudoran O, Feflea D, Balacescu L, Anghel A, Sirbu IO, Seclaman E and Marian C: Urinary microRNAs for prostate cancer diagnosis, prognosis, and treatment response: Are we there yet? Wiley Interdiscip Rev RNA 8, 2017.
9. Martignano F, Rossi L, Maugeri A, Gallà V, Conteduca V, De Giorgi U, Casadio V and Schepisi G: Urinary RNA-based biomarkers for prostate cancer detection. Clin Chim Acta 473: 96-105, 2017.
10. Mishra S, Yadav T and Rani V: Exploring miRNA based approaches in cancer diagnostics and therapeutics. Crit Rev Oncol Hematol 98: 12-23, 2016.
11. Han C, Shen JK, Hornicek FJ, Kan Q and Duan Z: Regulation of microRNA-1 (miR-1) expression in human cancer. Biochim Biophys Acta Gene Regul Mech 1860: 227-232, 2017.
12. Rigaud VO, Ferreira LR, Ayub-Ferreira SM, Ávila MS, Brandão SM, Cruz FD, Santos MH, Cruz CB, Alves MS, Issa VS, *et al*: Circulating miR-1 as a potential biomarker of doxorubicin-induced cardiotoxicity in breast cancer patients. Oncotarget 8: 6994-7002, 2017.
13. Wu X, Li S, Xu X, Wu S, Chen R, Jiang Q, Li Y and Xu Y: The potential value of miR-1 and miR-374b as biomarkers for colorectal cancer. Int J Clin Exp Pathol 8: 2840-2851, 2015.
14. Wei W, Leng J, Shao H and Wang W: MiR-1, a potential predictive biomarker for recurrence in prostate cancer after radical prostatectomy. Am J Med Sci 353: 315-319, 2017.
15. Di W, Li Q, Shen W, Guo H and Zhao S: The long non-coding RNA HOTAIR promotes thyroid cancer cell growth, invasion and migration through the miR-1-CCND2 axis. Am J Cancer Res 7: 1298-1309, 2017.
16. Xu W, Zhang Z, Zou K, Cheng Y, Yang M, Chen H, Wang H, Zhao J, Chen P, He L, *et al*: MiR-1 suppresses tumor cell proliferation in colorectal cancer by inhibition of Smad3-mediated tumor glycolysis. Cell Death Dis 8: e2761, 2017.
17. Shang A, Yang M, Shen F, Wang J, Wei J, Wang W, Lu W, Wang C and Wang C: MiR-1-3p Suppresses the proliferation, invasion and migration of bladder cancer cells by up-regulating sfrp1 expression. Cell Physiol Biochem 41: 1179-1188, 2017.
18. Liu R, Li J, Lai Y, Liao Y, Liu R and Qiu W: Hsa-miR-1 suppresses breast cancer development by down-regulating K-ras and long non-coding RNA MALAT1. Int J Biol Macromol 81: 491-497, 2015.
19. Chang YS, Chen WY, Yin JJ, Sheppard-Tillman H, Huang J and Liu YN: EGF Receptor promotes prostate cancer bone metastasis by downregulating mir-1 and activating TWIST1. Cancer Res 75: 3077-3086, 2015.
20. Stope MB, Stender C, Schubert T, Peters S, Weiss M, Ziegler P, Zimmermann U, Walther R and Burchardt M: Heat-shock protein HSPB1 attenuates microRNA miR-1 expression thereby restoring oncogenic pathways in prostate cancer cells. Anticancer Res 34: 3475-3480, 2014.
21. Deng M, Bragelmann J, Schultze JL and Perner S: Web-TCGA: An online platform for integrated analysis of molecular cancer data sets. BMC Bioinformatics 17: 72, 2016.
22. Anders S and Huber W: Differential expression analysis for sequence count data. Genome Biol 11: R106, 2010.
23. Dweep H and Gretz N: miRWalk2.0: A comprehensive atlas of microRNA-target interactions. Nat Methods 12: 697, 2015.
24. Shannon P, Markiel A, Ozier O, Baliga NS, Wang JT, Ramage D, Amin N, Schwikowski B and Ideker T: Cytoscape: A software environment for integrated models of biomolecular interaction networks. Genome Res 13: 2498-2504, 2003.
25. Tang Z, Li C, Kang B, Gao G, Li C and Zhang Z: GEPIA: A web server for cancer and normal gene expression profiling and interactive analyses. Nucleic Acids Res 45: W98-W102, 2017.
26. Pashaei E, Pashaei E, Ahmady M, Ozen M and Aydin N: Meta-analysis of miRNA expression profiles for prostate cancer recurrence following radical prostatectomy. PLoS One 12: e0179543, 2017.
27. Gravina GL, Festuccia C, Bonfili P, Di Staso M, Franzese P, Ruggieri V, Popov VM, Tombolini V, Masciocchi C, Carosa E, *et al*: Strategies for imaging androgen receptor signaling pathway in prostate cancer: Implications for hormonal manipulation and radiation treatment. Biomed Res Int 2013: 460546, 2013.
28. Attard G, Richards J and de Bono JS: New strategies in metastatic prostate cancer: Targeting the androgen receptor signaling pathway. Clin Cancer Res 17: 1649-1657, 2011.
29. Wang L, Song G, Chang X, Tan W, Pan J, Zhu X, Liu Z, Qi M, Yu J and Han B: The role of TXNDC5 in castration-resistant prostate cancer-involvement of androgen receptor signaling pathway. Oncogene 34: 4735-4745, 2015.
30. Ylitalo EB, Thysell E, Jernberg E, Lundholm M, Crnalic S, Egevad L, Stattin P, Widmark A, Bergh A and Wikström P: Subgroups of castration-resistant prostate cancer bone metastases defined through an inverse relationship between androgen receptor activity and immune response. Eur Urol 71: 776-787, 2017.
31. Pinto F, Pértega-Gomes N, Vizcaino JR, Andrade RP, Cárcano FM and Reis RM: Brachyury as a potential modulator of androgen receptor activity and a key player in therapy resistance in prostate cancer. Oncotarget 7: 28891-28902, 2016.
32. Ware KE, Somarelli JA, Schaeffer D, Li J, Zhang T, Park S, Patierno SR, Freedman J, Foo WC, Garcia-Blanco MA and Armstrong AJ: Snail promotes resistance to enzalutamide through regulation of androgen receptor activity in prostate cancer. Oncotarget 7: 50507-50521, 2016.
33. Wang Y, Ledet RJ, Imberg-Kazdan K, Logan SK and Garabedian MJ: Dynein axonemal heavy chain 8 promotes androgen receptor activity and associates with prostate cancer progression. Oncotarget 7: 49268-49280, 2016.
34. Jiang J, Jia P, Shen B and Zhao Z: Top associated SNPs in prostate cancer are significantly enriched in cis-expression quantitative trait loci and at transcription factor binding sites. Oncotarget 5: 6168-6177, 2014.
35. Eisermann K, Tandon S, Bazarov A, Brett A, Fraizer G and Piontkivska H: Evolutionary conservation of zinc finger transcription factor binding sites in promoters of genes co-expressed with WT1 in prostate cancer. BMC Genomics 9: 337, 2008.
36. Kojima S, Enokida H, Yoshino H, Itesako T, Chiyomaru T, Kinoshita T, Fuse M, Nishikawa R, Goto Y, Naya Y, *et al*: The tumor-suppressive microRNA-143/145 cluster inhibits cell migration and invasion by targeting GOLM1 in prostate cancer. J Hum Genet 59: 78-87, 2014.
37. Li SX, Tong YP, Xie XC, Wang QH, Zhou HN, Han Y, Zhang ZY, Gao W, Li SG, Zhang XC and Bi RC: Octameric structure of the human bifunctional enzyme PAICS in purine biosynthesis. J Mol Biol 366: 1603-1614, 2007.
38. Gallenne T, Ross KN, Visser NL, Salony, Desmet CJ, Wittner BS, Wessels LFA, Ramaswamy S and Peeper DS: Systematic functional perturbations uncover a prognostic genetic network driving human breast cancer. Oncotarget 8: 20572-20587, 2017.
39. Goswami MT, Chen G, Chakravarthi BV, Pathi SS, Anand SK, Carskadon SL, Giordano TJ, Chinnaiyan AM, Thomas DG, Palanisamy N, *et al*: Role and regulation of coordinately expressed de novo purine biosynthetic enzymes PPAT and PAICS in lung cancer. Oncotarget 6: 23445-23461, 2015.
40. Cifola I, Pietrelli A, Consolandi C, Severgnini M, Mangano E, Russo V, De Bellis G and Battaglia C: Comprehensive genomic characterization of cutaneous malignant melanoma cell lines derived from metastatic lesions by whole-exome sequencing and SNP array profiling. PLoS One 8: e63597, 2013.
41. Chakravarthi BV, Goswami MT, Pathi SS, Dodson M, Chandrashekar DS, Agarwal S, Nepal S, Hodigere Balasubramanya SA, Siddiqui J, Lonigro RJ, *et al*: Expression and role of PAICS, a de novo purine biosynthetic gene in prostate cancer. Prostate 77: 10-21, 2017.
42. Gall TM and Frampton AE: Gene of the month: E-cadherin (CDH1). J Clin Pathol 66: 928-932, 2013.
43. Li D, Zhang R, Jin T, He N, Ren L, Zhang Z, Zhang Q, Xu R, Tao H, Zeng G and Gao J: ADH1B and CDH1 polymorphisms predict prognosis in male patients with non-metastatic laryngeal cancer. Oncotarget 7: 73216-73228, 2016.
44. Jiao F, Hu H, Han T, Zhuo M, Yuan C, Yang H, Wang L and Wang L: Aberrant expression of nuclear HDAC3 and cytoplasmic CDH1 predict a poor prognosis for patients with pancreatic cancer. Oncotarget 7: 16505-16516, 2016.
45. Yu Q, Guo Q, Chen L and Liu S: Clinicopathological significance and potential drug targeting of CDH1 in lung cancer: A meta-analysis and literature review. Drugb Des Devel Ther 9: 2171-2178, 2015.
46. Huang R, Ding P and Yang F: Clinicopathological significance and potential drug target of CDH1 in breast cancer: A meta-analysis and literature review. Drug Des Devel Ther 9: 5277-5285, 2015.
47. Zeng W, Zhu J, Shan L, Han Z, Aerxiding P, Quhai A, Zeng F, Wang Z and Li H: The clinicopathological significance of CDH1 in gastric cancer: A meta-analysis and systematic review. Drug Des Devel Ther 9: 2149-2157, 2015.

48. Qiu LX, Li RT, Zhang JB, Zhong WZ, Bai JL, Liu BR, Zheng MH and Qian XP: The E-cadherin (CDH1)-160 C/A polymorphism and prostate cancer risk: A meta-analysis. Eur J Hum Genet 17: 244-249, 2009.
49. Ren H, Du P, Ge Z, Jin Y, Ding D, Liu X and Zou Q: TWIST1 and BMI1 in cancer metastasis and chemoresistance. J Cancer 7: 1074-1080, 2016.
50. Liu H, Wang H, Liu X and Yu T: miR-1271 inhibits migration, invasion and epithelial-mesenchymal transition by targeting ZEB1 and TWIST1 in pancreatic cancer cells. Biochem Biophys Res Commun 472: 346-352, 2016.
51. Li L and Wu D: miR-32 inhibits proliferation, epithelial-mesenchymal transition, and metastasis by targeting TWIST1 in non-small-cell lung cancer cells. Onco Targets Ther 9: 1489-1498, 2016.
52. Ávila-Moreno F, Armas-López L, Álvarez-Moran AM, López-Bujanda Z, Ortiz-Quintero B, Hidalgo-Miranda A, Urrea-Ramírez F, Rivera-Rosales RM, Vázquez-Manríquez E, Peña-Mirabal E, *et al*: Correction: Overexpression of MEOX2 and TWIST1 is associated with H3K27me3 levels and determines lung cancer chemoresistance and prognosis. PLoS One 11: e0146569, 2016.
53. Wang T, Hou J, Li Z, Zheng Z, Wei J, Song D, Hu T, Wu Q, Yang JY and Cai JC: miR-15a-3p and miR-16-1-3p negatively regulate twist1 to repress gastric cancer cell invasion and metastasis. Int J Biol Sci 13: 122-134, 2017.
54. Cao C, Sun D, Zhang L and Song L: miR-186 affects the proliferation, invasion and migration of human gastric cancer by inhibition of Twist1. Oncotarget 7: 79956-79963, 2016.
55. Matsusaka S, Zhang W, Cao S, Hanna DL, Sunakawa Y, Sebio A, Ueno M, Yang D, Ning Y, Parekh A, *et al*: TWIST1 polymorphisms predict survival in patients with metastatic colorectal cancer receiving first-line bevacizumab plus oxaliplatin-based chemotherapy. Mol Cancer Ther 15: 1405-1411, 2016.
56. Zhu DJ, Chen XW, Zhang WJ, Wang JZ, Ouyang MZ, Zhong Q and Liu CC: Twist1 is a potential prognostic marker for colorectal cancer and associated with chemoresistance. Am J Cancer Res 5: 2000-2011, 2015.
57. Yusup A, Huji B, Fang C, Wang F, Dadihan T, Wang HJ and Upur H: Expression of trefoil factors and TWIST1 in colorectal cancer and their correlation with metastatic potential and prognosis. World J Gastroenterol 23: 110-120, 2017.
58. Malek R, Gajula RP, Williams RD, Nghiem B, Simons BW, Nugent K, Wang H, Taparra K, Lemtiri-Chlieh G, Yoon AR, *et al*: TWIST1-WDR5-hottip regulates hoxa9 chromatin to facilitate prostate cancer metastasis. Cancer Res 77: 3181-3193, 2017.
59. Zhao X, Deng R, Wang Y, Zhang H, Dou J, Li L, Du Y, Chen R, Cheng J and Yu J: Twist1/Dnmt3a and miR186 establish a regulatory circuit that controls inflammation-associated prostate cancer progression. Oncogenesis 6: e315, 2017.
60. Zhao X, Wang Y, Deng R, Zhang H, Dou J, Yuan H, Hou G, Du Y, Chen Q and Yu J: miR186 suppresses prostate cancer progression by targeting Twist1. Oncotarget 7: 33136-33151, 2016.
61. Cho KH, Choi MJ, Jeong KJ, Kim JJ, Hwang MH, Shin SC, Park CG and Lee HY: A ROS/STAT3/HIF-1α signaling cascade mediates EGF-induced TWIST1 expression and prostate cancer cell invasion. Prostate 74: 528-536, 2014.
62. Gajula RP, Chettiar ST, Williams RD, Thiyagarajan S, Kato Y, Aziz K, Wang R, Gandhi N, Wild AT, Vesuna F, *et al*: The twist box domain is required for Twist1-induced prostate cancer metastasis. Mol Cancer Res 11: 1387-1400, 2013.
63. Cho KH, Jeong KJ, Shin SC, Kang J, Park CG and Lee HY: STAT3 mediates TGF-β1-induced TWIST1 expression and prostate cancer invasion. Cancer Lett 336: 167-173, 2013.
64. Xu Z, Zhou Y, Cao Y, Dinh TL, Wan J and Zhao M: Identification of candidate biomarkers and analysis of prognostic values in ovarian cancer by integrated bioinformatics analysis. Med Oncol 33: 130, 2016.
65. Ho JR, Chapeaublanc E, Kirkwood L, Nicolle R, Benhamou S, Lebret T, Allory Y, Southgate J, Radvanyi F and Goud B: Deregulation of Rab and Rab effector genes in bladder cancer. PLoS One 7: e39469, 2012.
66. Gilling CE, Mittal AK, Chaturvedi NK, Iqbal J, Aoun P, Bierman PJ, Bociek RG, Weisenburger DD and Joshi SS: Lymph node-induced immune tolerance in chronic lymphocytic leukaemia: A role for caveolin-1. Br J Haematol 158: 216-231, 2012.
67. Abdelgawad IA, Radwan NH and Hassanein HR: KIAA0101 mRNA expression in the peripheral blood of hepatocellular carcinoma patients: Association with some clinicopathological features. Clin Biochem 49: 787-791, 2016.
68. Yuan RH, Jeng YM, Pan HW, Hu FC, Lai PL, Lee PH and Hsu HC: Overexpression of KIAA0101 predicts high stage, early tumor recurrence, and poor prognosis of hepatocellular carcinoma. Clin Cancer Res 13: 5368-5376, 2007.
69. Liu L, Liu Y, Chen X, Wang M, Zhou Y, Zhou P, Li W and Zhu F: Variant 2 of KIAA0101, antagonizing its oncogenic variant 1, might be a potential therapeutic strategy in hepatocellular carcinoma. Oncotarget 8: 43990-44003, 2017.
70. Zhu K, Diao D, Dang C, Shi L, Wang J, Yan R, Yuan D and Li K: Elevated KIAA0101 expression is a marker of recurrence in human gastric cancer. Cancer Sci 104: 353-359, 2013.
71. Zhang CF, Xia YH, Zheng QF, Li ZJ, Guo XH, Zhou HC, Zhang LL, Dong LP and Han Y: Effects of KIAA0101 expression on proliferation and invasion of gastric carcinoma MKN-45 cells. Zhonghua Bing Li Xue Za Zhi 41: 553-557, 2012 (In Chinese).
72. Kato T, Daigo Y, Aragaki M, Ishikawa K, Sato M and Kaji M: Overexpression of KIAA0101 predicts poor prognosis in primary lung cancer patients. Lung Cancer 75: 110-118, 2012.
73. Cheng Y, Li K, Diao D, Zhu K, Shi L, Zhang H, Yuan D, Guo Q, Wu X, Liu D and Dang C: Expression of KIAA0101 protein is associated with poor survival of esophageal cancer patients and resistance to cisplatin treatment in vitro. Lab Invest 93: 1276-1287, 2013.
74. Fan S, Li X, Tie L, Pan Y and Li X: KIAA0101 is associated with human renal cell carcinoma proliferation and migration induced by erythropoietin. Oncotarget 7: 13520-13537, 2016.